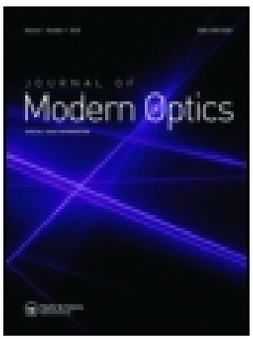

Journal of Modern Optics

ISSN: 0950-0340 (Print) 1362-3044 (Online) Journal homepage: http://www.tandfonline.com/loi/tmop20

Limits to remote molecular detection via coherent anti-Stokes raman spectroscopy using a maximal coherence control technique

Gengyuan Liu, Frank A Narducci & Svetlana A Malinovskaya

To cite this article: Gengyuan Liu, Frank A Narducci & Svetlana A Malinovskaya (2018): Limits to remote molecular detection via coherent anti-Stokes raman spectroscopy using a maximal coherence control technique, Journal of Modern Optics, DOI: 10.1080/09500340.2018.1514084

To link to this article: https://doi.org/10.1080/09500340.2018.1514084

Published online: 05 Sep 2018.

Submit your article to this journal

Article views: 3

View Crossmark data

Full Terms & Conditions of access and use can be found at
http://www.tandfonline.com/action/journalInformation?journalCode=tmop20

JOURNAL OF MODERN OPTICS
https://doi.org/10.1080/09500340.2018.1514084

Taylor & Francis
Taylor & Francis Group

Check for updates

Limits to remote molecular detection via coherent anti-Stokes raman spectroscopy using a maximal coherence control technique

Gengyuan Liu[a], Frank A Narducci[b] and Svetlana A Malinovskaya[a]

[a]Department of Physics, Stevens Institute of Technology, Hoboken, USA; [b]Department of Physics, Naval Postgraduate School, Monterey, USA

ABSTRACT

The demand for remote molecular detection has been rising in recent years. The technique of coherent anti-Stokes Raman spectroscopy (CARS) has become one of the most optimal methods due to its high efficiency, fast response time and ease of use. In this article, we estimate the number of detectable photons from a CARS signal by using a semiclassical nonlinear optics approach. Several key parameters and their effect on the signal are studied in the following discussion. We also provide a method to prepare the maximum coherence between vibrational states in an effective two level system.

ARTICLE HISTORY
Received 14 March 2018
Accepted 13 August 2018

KEYWORDS
Remote detection; coherent anti-Stokes raman scattering (CARS); optical frequency comb; coherent control; maximum coherence

Advances in ultrafast laser technology have brought new opportunities and challenges to investigations of light-matter interaction as well as applications at the frontier of science and technology. Owing to the need for identification of chemicals and hazardous contaminants, techniques of remote molecular detection and its attendant problems are rapidly evolving thanks to new developments in super-resolution methods. Latest advancements in this field include trace chemical sensing via surface enhanced infrared absorption through coupling of phonon and plasmon resonance (*1*), signal amplification for molecular detection by surface-enhanced Raman scattering (*2*), and Coherent anti-Stokes Raman Spectroscopy (CARS) for standoff detection (*3–5*).

An optical frequency comb is a new and unique spectroscopic tool that is added to the high resolution analysis of atoms and molecules toolbox in both theoretical and experimental research areas (*6–11*). Recently, the frequency comb was successfully implemented in quantum control of atomic and molecular dynamics owing to a large number of control parameters, which may be easily addressed including the pulse duration, repetition rate, peak intensity and spectral phase modulation (*12–15*). We implement this new approach for the coherence control between vibrational states in the last part of this paper.

Since the backscattered signal of CARS is orders of magnitude stronger than spontaneous Raman emission, it can be an extremely useful tool for remote identification of air particles. A sufficiently strong CARS signal in the backward direction can be provided by maximizing quantum coherence in a molecular system, which dramatically increases the nonlinear response of a medium. Maximum coherence between vibrational levels in molecules can be created with Femtosecond Adaptive Spectroscopic Techniques (FAST) applied to CARS. FAST CARS is based on shaping the phase and amplitude of femtosecond pulses to manipulate their interaction with the molecules. The adiabatic regime of this interaction is particularly advantageous because it can be easily implemented in experimental setups without the need for explicitly tuning lasers into resonance and choosing the exact magnitude of the field intensity.

CARS is a third order nonlinear optical process involving three laser beams: the pump, the Stokes and the probe at frequencies, ω_p, ω_s and ω_{pr} respectively, Figure 1. Two, two-level systems represent Raman active vibrational modes. We aim to produce and detect a signal from the $|1> - |2>$ two-level system, the $|3> - |4>$ two-level system represents an alternative Raman active mode, the signal from which we do not want to receive, therefore it should not be excited. It may also relate to the non-resonant background of the four-wave mixing process.The three incident beams interact with a sample and generate the anti-Stokes field at frequency $\omega_{as} = \omega_p + \omega_{pr} - \omega_s$, which is blue shifted, away from the (auto)fluorescent background.

CONTACT Svetlana A Malinovskaya smalinov@stevens.edu Department of Physics, Stevens Institute of Technology, Hoboken, NJ 07030, USA

© 2018 Informa UK Limited, trading as Taylor & Francis Group.

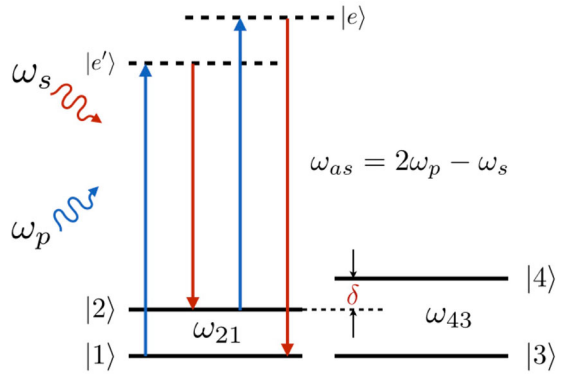

Figure 1. Schematic of CARS: the pump (ω_p) and the Stokes (ω_s) fields interact with the ground $|1\rangle$ and the excited vibrational state $|2\rangle$ through the electronic excited state; the probe field, which has the same frequency as the pump, interacts with the induced coherence $|\rho_{21}|$ to generate the anti-Stokes field at frequency $\omega_{as} = \omega_p + \omega_{pr} - \omega_s$. The ω_{43} is the frequency of the alternative vibrational mode to be suppressed. It also represents the background. The δ is the two-photon detuning, which may be as small as 1 cm^{-1} or less.

Because CARS is a coherent process, the CARS signal is an orders of magnitude higher than the spontaneous Raman scattering signal and, in addition, has directional selectivity defined by the phase-matching condition. This condition requires the wave vectors of the incoming waves and of outgoing waves relate as $\mathbf{k_{as}} = \mathbf{k_p} + \mathbf{k_{pr}} - \mathbf{k_s}$, meaning that the laser beams have to be properly aligned.

Based on a semiclassical approach, we estimated the feasibility of FAST CARS for a real-time remote detection of hazardous microparticles in atmosphere. We also evaluated the range of distances for typical species based on the parameters of a typical laser system that drive the limits. We rely on a semiclassical theory of nonlinear scattering introduced in (*16*) to estimate the number of detectable photons from molecules at a predetermined distance. In (*16*), the integral solution of the nonlinear scattering by the particle is obtained from the inhomogeneous vector wave equation with the right side in the form of induced polarization as a source to generate the CARS signal. Reflection and refraction due to the linear response of the signal are implicitly accounted for in the anti-Stokes coherence obtained from the Bloch equations. The Lorenz-Mie theory is implemented to study the inhomogeneous spatial distributions on the incident fields as the results of refraction and internal reflection in a single bacterial spore. The strength of the backward signal from a single spore was estimated by plotting the anti-Stokes signal as a function of observation angle, Figure 3 in (*16*). It shows that the backscattered signal is almost as strong as the forward signal. The ratio of the signal intensity to probe intensity is plotted for inhomogeneous fields within the spore due to lensing and focusing by the spore. For remote molecular detection, the situation in the detection area that contains target molecules could be extremely complex. For example, detection target could be tiny droplets of molecules, or just an open area containing molecules. In the droplets case, a similar response could be expected as for the anthrax, because a tiny droplet having the size similar to the probing wavelength would interact with the field similarly to a single spore. In the second, the homogeneous case of a dense cloud of molecules, the theory in (*16*) can be used to provide a sufficiently meaningful magnitude of detectable signal, even though the phase matching condition is tight (*17*).

We investigated methanol as a prototypical molecule. The molecule of methanol has two Raman active vibrational modes: the symmetric 2837 cm^{-1} (85.05 THz) mode and asymmetric 2942 cm^{-1} (88.20 THz) stretch mode. The frequency of these vibrational modes is slightly different, so that testing the chemical selectivity of detection is possible. We estimated the density of photons scattered in the backward direction, and calculated the irradiance that can be detected by a detector placed 1 km away from the target molecules. The ratio of the backscattered number of photons to the number of the probe photons (*16*) is

$$\frac{n_4(R,\omega_{ac})}{n_3} = \frac{\epsilon}{2\pi}\left(\frac{d}{w}\right)^2 \int_0^{2\pi} \frac{\mathcal{I}_4(R,\omega_{ac})_{\Theta=0(\pi)}}{\mathcal{I}_3(\omega_{ac})}\,\mathrm{d}\Phi \tag{1}$$

where ϵ is the detector efficiency, d is the detector's diameter and w is the laser beam diameter. Θ is the angle of scattering, $\Theta = 0$ for forward direction and $\Theta = \pi$ for backward direction. The intensity ratio in Equation (1) is

$$\frac{\mathcal{I}_4(\boldsymbol{R},\omega_{ac})_{\Theta=0(\pi)}}{\mathcal{I}_3(\omega_{ac})} = |\hat{\epsilon}_s|^2\left(\frac{3}{8\pi R}\lambda\frac{\gamma_r}{\gamma_{ac}}N|\rho_{21}(0)|F\right)^2 \tag{2}$$

Here, ϵ_s is the polarization of the signal field, R is the distance between detector and the target molecule, λ is the anti-Stokes wavelength, γ_r is the radiative decay rate and γ_{ac} is the decoherence rate, N is the number of target molecules and $|\rho_{21}|$ is the coherence between vibrational levels.

The parameter F is the geometrical and orientation factor, which depends on the target area volume and the phase mismatch. For a perfect phase matching condition $F = 1$, which we used in our calculations because it is naturally provided by the size of the methanol molecule having molecular diameter $\rho_0 = 10^{-9}$ m and the working anti-Stokes wavelength $\lambda = 0.65\,\mu$m, satisfying the required condition $\lambda \gg \rho_0$. We have made a series of test calculations to analyze the dependance of the ratio of the

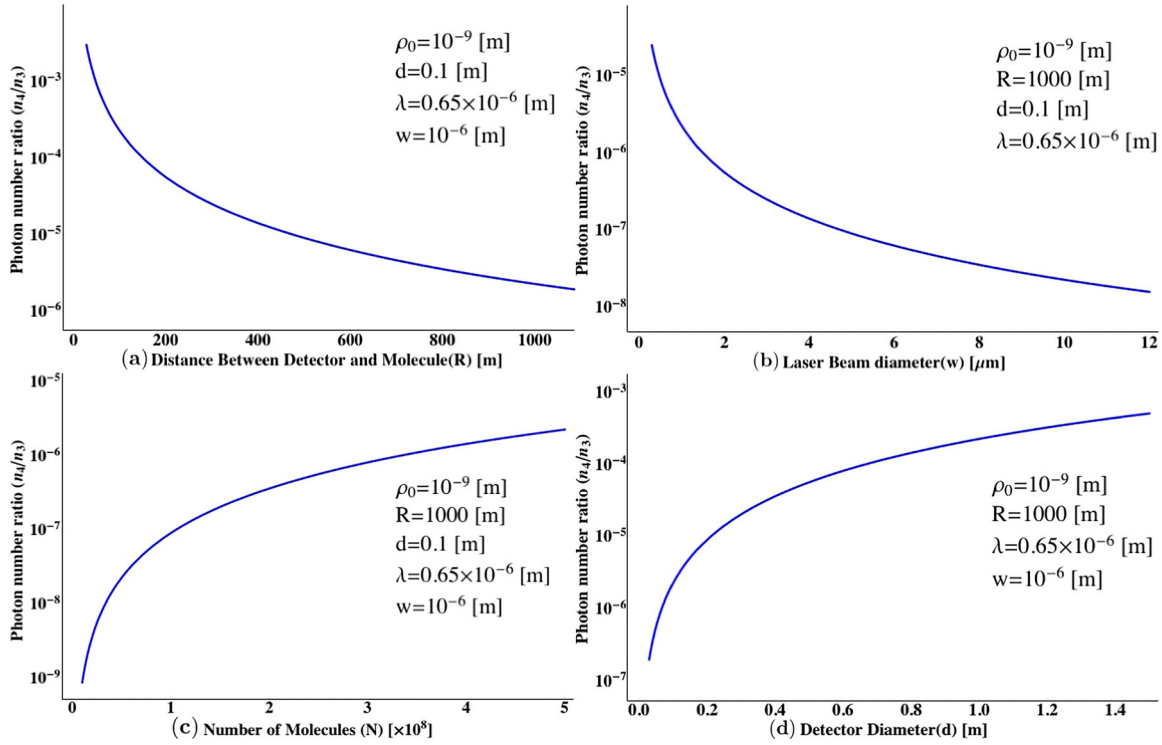

Figure 2. The ratio of the number of incident photons to the anti-Stokes backscattered photons as a function of (a) distance between detector and molecule, (b) the laser beam diameter, (c) number of target molecules and (d) the detector diameter.

incident to the backscattered photons as a function of the distance between the detector and the molecule (R), the laser beam diameter (w), and the detector diameter (d). The results are presented in the Figure 2.

Based on the above calculations, we have made the following estimates. Suppose, the detector has a diameter $d = 0.1$ m and it is placed $R = 1$ km away. The detector efficiency is $\epsilon = 0.1$, radiative decay is $\gamma_r = 10^8\ \mathrm{s}^{-1}$, decoherence rate is $\gamma_{ac} = 2.5 \times 10^{13}\ \mathrm{s}^{-1}$, the number of molecules $N = 5 \times 10^8$ and the laser beam diameter is $w = 1\,\mu$m (*16*). The coherence between vibrational levels is maximal, $|\rho_{21}| = 0.5$. For these values of parameters, the ratio between the number of incident photons and backscattered anti-Stokes photons n_4/n_3 is about 10^{-5}. The pulse energy used in this simulation is 0.6 nJ and wavelength is $\lambda = 800$ nm. As a result, the number of backscattered photons is

$$N_{3\,per\,pulse} = \frac{E_0}{h \cdot \frac{c}{\lambda}} = 2 \times 10^9, \tag{3}$$

giving the number of anti-Stokes photons per pulse $n_{4\ per\ pulse} = 2 \times 10^4$. If the pulse repetition rate is 1 GHz, the number of anti-Stokes photons per second is about 2×10^{13}, which is equivalent to 2 μW power and is sufficient for detection.

The pulse parameters are relevant for an experimental setup in the laboratory. We use a Coherent Verdi-pumped GigiOptics mode-locked Titanium Sapphire Laser with a repetition rate of 1 GHz. The pulse width of a single pulse is approximately 55 fsec, as measured by a symmetric Michelson interferometer (*18*). The laser spectrum is centered around $\lambda = 825$ nm with a full-width half-maximum bandwidth of 25 nm. The total average mode-locked power can reach 1 Watt.

In the ratio of the incident to anti-Stokes backscattered photons in Equation (1), one of the key parameters is the coherence between vibrational levels $|\rho_{21}|$. This parameter can be controlled by an input pulse, and its value can be maximized in order to maximize the $n_4(R, \omega_{ac})/n_3$. A series of calculations for the dynamics in the target molecule, methanol, is presented below, which demonstrate the usefulness of the pulsed radiation with values for the relevant parameters listed above for maximizing vibrational coherence. Consider a three level system consisting of two vibrational states of the ground electronic state and one excited electronic-vibrational state in a molecule. This molecule interacts with the pump and Stokes pulses, which induce molecular dynamics and population transfer. The pulses are chosen to be transform-limited since we only estimate the field intensity and frequency at this point; the pulses read

$$E_{p(s)} = E_{p(s)0}\, \mathrm{e}^{-t^2/\tau^2} \cos(\omega_{p(s)} t), \tag{4}$$

where $E_{p(s)0}$ is the peak value of the field intensity, τ is the pump or Stokes pulse duration, and $\omega_{p(s)}$ is the carrier

frequency of the pump and Stokes pulse. The light-matter Hamiltonian in the interaction representation reads

$$\hat{H} = \hbar \begin{pmatrix} 0 & 0 & \frac{\Omega_p(t)}{2} e^{i\omega_1 t} \\ 0 & 0 & \frac{\Omega_s(t)}{2} e^{-i(\omega_p-\omega_s-\omega_s)t} \\ \frac{\Omega_p^*(t)}{2} e^{-i\omega_1 t} & \frac{\Omega_s^*(t)}{2} e^{i(\omega_p-\omega_s-\omega_s)t} & \omega_3-\omega_p \end{pmatrix}. \tag{5}$$

Here $\Omega_{p(s)} = -(\mu/\hbar)E_{p(s)0}\, e^{-t^2/\tau^2}$ is the Rabi frequency, and μ is the transition dipole moment, which we assume to be the same for both transitions for simplicity. If the field and system parameters satisfy the condition that the one-photon detuning $\Delta \gg \Omega_{p(s)}$, where $\Delta = \omega_{31} - \omega_p$, then the excited level is scarcely populated during the interaction. It means the change of population amplitude of the excited level in time is negligible. Then the excited state can be adiabatically eliminated and the system reduces to an effective two-level system, for which the Hamilton is

$$\hat{H}_{eff} = \hbar \begin{pmatrix} -\frac{|\Omega_p(t)|^2}{4\Delta} & -\frac{\Omega_p(t)\Omega_s^*(t)}{4\Delta} e^{i\delta t} \\ -\frac{\Omega_p^*(t)\Omega_s(t)}{4\Delta} e^{-i\delta t} & -\frac{|\Omega_s(t)|^2}{4\Delta} \end{pmatrix}. \tag{6}$$

Here, $\delta = (\omega_p - \omega_s - \omega_2 + \omega_1)$ is the two-photon detuning. The coherence between the vibrational levels can be studied by solving the time-dependent Schrödinger equation numerically. To simplify the solution, we choose the resonance condition, ($\delta = 0$), and assume the peak value of the Rabi frequency is the same for both the pump and Stokes pulses, $\Omega_{p0} = \Omega_{s0}$. We define the effective Rabi frequency as $\Omega_{eff} \equiv (\Omega_p(t)\Omega_s^*(t))/4\Delta$.

The population and coherence dynamics in the effective two-level system are shown in Figure 3 as a function of the peak effective Rabi frequency Ω_{eff}. It shows Rabi oscillations with periodic complete population transfer to the upper vibrational state following the pulse area solution. The first complete population transfer to the target, vibrationally excited state $|2\rangle$ happens at $\Omega_{eff} =$ 22.5 THz, which has the π pulse area. This figure also shows the points of the maximum coherence, ($|\rho_{21}| =$ 0.5), between two vibrational states, which occurs exactly at the crossings of two populations when their value is equal to1/2.

The peak value of the Rabi frequency of both the pump and Stokes pulses at the first maximum coherence is $\Omega_R = 212$ THz and at the first population inversion is $\Omega_R = 300$ THz, which are equivalent to the peak field amplitude 6.7×10^7 V · cm^{-1} and 9.48×10^7 V · cm^{-1} respectively for the effective transition dipole equal to 1 D. The population transfer and the maximum coherence could also be achieved by a lower peak field

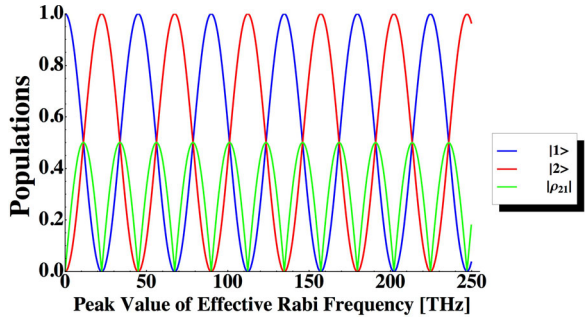

Figure 3. Population dynamics in the effective two-level system. The single pulse duration is $\tau = 55.8$ [fs], the one-photon detuning $\Delta = 1000$ [THz] and the two-photon detuning $\delta = 0$.

amplitude of the pulse via the pulse train technique. A phase-locked pulse train, which forms an optical frequency comb, provides a coherent population transfer to the target state in a piecewise manner. It induces two-photon transitions in a molecular system and creates a quasi-dark state, which allows to efficiently mitigate decoherence (*19*). As an example, we used the peak value of 2.275×10^7 V · cm^{-1} of a Ti-Sapphire laser (*20*) in our calculation, which is equivalent to the peak Rabi frequency 72 THz. Under such conditions, the maximum coherence is accumulated by the pulse train having 8 pulses, while the full population transfer occurs after 17 pulses, see Figure 4.

In conclusion, we have analyzed a new technique based on the coherent anti-Stokes Raman spectroscopy to remotely identify traces of target air molecules, using methanol as a surrogate molecule. An estimation of the backscattered CARS signal is made based on the semiclassical theory and a series of key parameters are analyzed that impact the number the anti-Stokes backscattered photons. We also have demonstrated the technique in an effective two-level system to control the

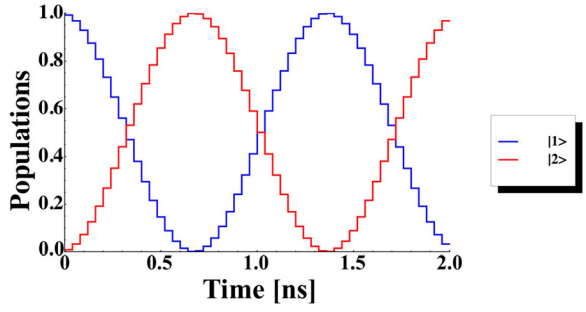

Figure 4. The population dynamics in the effective two-level system as a function of time for the peak value of the field amplitude 2.275×10^7 V · cm^{-1} corresponding to the $\Omega_{eff} = 1.3$ THz. The single pulse duration is $\tau = 55.8$ fs, the one-photon detuning $\Delta = 1000$ THz, the two-photon detuning $\delta = 0$. The pulse train period is 40 ps. The crossing of populations indicating the maximum coherence occurs after 8 pulses.

coherence between the vibrational states. A method of implementing a coherent pulse train is presented, which paves the path to control the excitations by an optical frequency comb. The results of the numerical calculations have shown that the coherence between the vibrational states can be maximized by carefully chosen parameters, and the CARS technique is a promising tool for the remote molecular detection.

Acknowledgements

The authors gratefully acknowledge the support from the Office of Naval Research.

Disclosure statement

No potential conflict of interest was reported by the authors.

Funding

This work was supported by Office of Naval Research [N00014-17-1-2523].

References

(1) Anderson, M.S. Surface enhanced infrared absorption by coupling phonon and plasma resonance. *App. Phys. Lett* . **2005,** *87*, 144102. https://doi.org/10.1063/1.2077838.
(2) Shi C.; Yan H.; Gu C.; Ghosh D.; Seballos L.; Chen S.; Zhang J.Z.; Chen B. *App. Phys. Lett.* **2008,** *92,* 103107.
(3) Katz O.; Natan A.; Silberberg Y.; Rosenwaks S. *App. Phys. Lett.* **2008,** *92,* 171116.
(4) Li H.; Harris A.; Xu B.; Wrzesinski P.J.; Lozovoy V.V.; Dantus M. *Opt. Expr.* **2008,** *16,* 5499.
(5) Beadie G.; Reintjes J.; Bashkansky M.; Opatrny T.; Scully M.O. *J. Mod. Opt.* **2003,** *50,* 2361.
(6) Cundiff S.T.; Ye J. *Rev. Mod. Phys.* **2003,** *75,* 325.
(7) Ozawa A.; Rauschenberger J.; Gohle Ch.; Herrmann M.; Walker D.R.; Pervak V.; Fernandez A.; Graf R.; Apolonski A.; Holzwarth R.; Krausz F.; Ha"nsch T.W.; Udem Th. *Phys. Rev. Lett.* **2008,** *100,* 253901.
(8) Wu J.; Qi H.; Zeng H. *Phys. Rev. A* **2008,** *77,* 053412.
(9) Gebs R.; Dekorsy T.; Diddams S.A.; Bartels A. *Opt. Expr.* **2008,** *16,* 5397.
(10) Savchenkov A.A.; Matsko A.B.; Ilchenko V.S.; Solomatine I.; Seidel D.; Maleki L. *Phys. Rev. Lett.* **2008,** *101,* 093902.
(11) Thorpe M.J.; Moll K.D.; Jones R.J.; Safdi B.; Ye J. *Science* **2006,** *311,* 1595.
(12) Peér A.; Shapiro E.A.; Stowe M.C.; Shapiro M.; Ye J. *Phys. Rev. Lett.* **2007,** *98* (4), 113004.
(13) Shapiro E.A.; Milner V.; Menzel-Jones C.; Shapiro M. *Phys. Rev. Lett.* **2007,** *99* (4), 033002.
(14) Shi S.; Woody A.; Rabitz H. *J. Chem. Phys.* **1988,** *88,* 6870.
(15) Shi S.; Rabitz H. *Chem. Phys.* **1989,** *139,* 185.
(16) Ooi C.H.R.; Beadie G.; Kattawar G.W.; Reinjes J.F.; Rostovtsev Y.; Zubairy M.S.; Scully M.O. *Phys. Rev. A* **2005,** *72,* 023807.
(17) Yuan L.; Lanin A.A.; Jha P.K.; Traverso A.J.; Voronine D.V.; Dorfman K.E.; Fedotov A.B.; Welch G.R.; Sokolov A.V.; Zheltikov A.M.; Scully M.O. *Laser Phys. Lett.* **2011,** *8,* 736.
(18) Trebino, R. *Frequency-Resolved Optical Gating: The Measurement of Ultrashort Laser Pulses*; Springer: New York, 2000. Chapter 4.
(19) Malinovskaya S.A.; Liu G. *Chem. Phys. Lett.* **2016,** *664,* 1.
(20) DeSavage S.A. Private communication, 2016.